Supporting Information

Theuser et al. 10.1073/pnas.1524616113

SI Results

Additional Gel-Based Disruption Assays. Initial gel-based disruption assays included an excess of nonradioactive U4 snRNA trap over Snu13 to sequester possibly dissociated proteins, which prevented Snu13 binding to the maximally expected radioactive U4 snRNA product, but not the formation of a Prp31–Snu13–U4 snRNA complex. Larger amounts of U4 snRNA trap sequestered the helicase and interfered with unwinding. We therefore conducted the above experiments including larger amounts of unlabeled U4 5′SL (U4 residues 20–53), which lacks the Brr2-binding U4 3′–single-stranded region. U4 5′SL prevented rebinding of 90 ± 1% of Snu13 and Prp31 to radiolabeled U4 snRNA (Fig. S4 *A* and *B*, compare lanes 3 and 4). Thus, if Prp31–Snu13–U4 snRNA complex formation was due to rebinding of the proteins after their displacement, we would expect a maximum of 10 ± 1% Prp31-Snu13-U4 snRNA product relative to free U4. Instead, we observed 28 ± 3% relative Prp31–Snu13–U4 snRNA complex after 68 min during Brr2-Jab1$^{\Delta C}$–mediated U4/U6 di-snRNP disruption (Fig. S4*A*, lane 11; quantification in Fig. S4*C*). Formation of the Prp31-Snu13-U4 RNP was again ATP-dependent (Fig. S4*A*, lanes 12–18). The large amounts of trap led to some initial Brr2-independent liberation of free U4/U6 di-snRNA (Fig. S4 *A*, lanes 5–11 and 12–18 and Fig. S4*B*, lanes 5–11), which is efficiently unwound by Brr2-Jab1$^{\Delta C}$ (Fig. S1). The amount of U4/U6 di-snRNA due to this side reaction fully accounts for the U4 snRNA product formed during unwinding by Brr2-Jab1$^{\Delta C}$ (Fig. S4*D*).

Monitoring U4/U6 Disruption via FRET. Because Snu13 and Prp31 do not stably interact in the absence of U4 or U4/U6 (29), we monitored whether Brr2-mediated U4/U6 disruption leads to spatial separation of the proteins, which would indicate their displacement from the RNAs. We generated variants of Snu13 and Prp31 bearing single modifiable cysteine residues that allowed labeling with Cy3 and Cy5 dyes. Labeling did not alter the RNA-binding properties of the proteins. We then tested binding, dissociation, and possible Brr2-mediated displacement using a stopped-flow apparatus. Due to the omission of glycerol, heparin, and BSA in this setup, reactions were considerably faster than in the gel-based assays. As expected from Snu13 and Prp31 binding close to each other on U4/U6, addition of Prp31^{Cy3} to Snu13^{Cy5}–U4/U6 or Brr2–Jab1$^{\Delta C}$–Snu13^{Cy5}–U4/U6 complexes gave rise to a FRET signal (Fig. S5*A*). In the absence of ATP, addition of a fivefold excess of unlabeled Prp31 to a Brr2-Jab1$^{\Delta C}$-Prp31^{Cy3}-Snu13^{Cy5}-U4/U6 RNP led to a time-dependent reduction of the FRET signal, representing spontaneous dissociation of Prp31^{Cy3} and its replacement by unlabeled Prp31 (Fig. S5*B*). Notably, Prp31^{Cy3} dissociation rates were very similar in the presence of ATP (Fig. S5*B*), although Brr2-Jab1$^{\Delta C}$ unwound 69 ± 5% of U4/U6 di-snRNA within 5 s under ATP conditions (Fig. S5*C*). These results again suggest that Brr2-Jab1$^{\Delta C}$–mediated U4/U6 disruption does not involve active displacement of either protein from the RNAs.

SI Discussion

After release of U6 snRNA by Brr2-mediated unwinding of stem I and conformational switching of U6, Brr2 might still remain associated with U4 and, upon further ATP-driven translocation on U4, would encounter bound Prp31 and Snu13. Several mechanisms can be envisaged by which Prp31 and Snu13 could counteract their own displacement from U4 snRNA. Single-molecule analyses have shown that the coaxial stack of U4/U6 stems I and II with the U4 5′ SL in a perpendicular orientation as seen in cryo-EM structures of U4/U6•U5 tri-snRNPs (22, 31, 58) is also adopted by isolated U4/U6 di-snRNA and is stabilized by binding of Snu13, Prp31, and a Prp3/Prp4 complex (39). U4/U6 di-snRNA thus exhibits a kink between stem I and the U4 5′SL, which could prevent or delay Brr2 from translocating into the U4 5′SL and favor its dissociation before it can displace Prp31 and Snu13. However, as shown here, Brr2 also does not seem to dislodge Prp31 and Snu13 from U4 snRNA alone, where this conformational restraint most likely does not exist. Because Prp31 and Snu13 bind U4 snRNA cooperatively (29, 30, 39), the two proteins together might present a stable roadblock that prevents translocation of Brr2 into the U4 5′ SL. At the point when the helicase encounters these physical obstacles, it apparently has unwound a sufficient fraction of U4/U6 to allow U6 snRNA to switch into an alternative conformation. In either scenario, Prp31 and Snu13 acts as a gatekeeper that prevents Brr2 from translocating into the U4 5′SL.

SI Materials and Methods

Protein Production and Purification. A synthetic gene encoding yeast Brr2$^{271\text{-end}}$ was cloned in-frame with an N-terminal His$_{10}$-tag and a tobacco etch virus (TEV) protease cleavage site into a modified pFL vector. Tn7 transposition was used to transfer the expression construct into an EMBacY baculovirus genome, maintained as a bacterial artificial chromosome (bacmid) in *E. coli*. Sf9 cells (Invitrogen) were transfected with the purified recombinant bacmid, and the first virus generation (V_0) was harvested and further amplified in Sf9 cells (Invitrogen). A high-titer virus generation (V_1) was used for large-scale expression in High Five Cells (Invitrogen). The cell pellet of an 800-mL culture was resuspended in 50 mM Hepes (pH 8.0), 20% (vol/vol) glycerol, 600 mM NaCl, 10 mM imidazole, 1.5 mM $MgCl_2$, 0.05% Nonidet P-40, and 2 mM β-mercaptoethanol supplemented with EDTA-free protease inhibitor (Roche). Cells were lysed by sonication for 30 min in a Sonopuls Ultrasonic Homogenizer HD 3100 (Bandelin; amplitude of 50%, pulse on for 0.5 s, pulse off for 2.0 s). Brr2 was affinity-captured on a 5-mL HisTrap FF column (GE Healthcare) equilibrated in 50 mM Hepes (pH 8.0), 20% (vol/vol) glycerol, 600 mM NaCl, 10 mM imidazole, and 2 mM β-mercaptoethanol, and eluted with a linear gradient from 10 to 250 mM imidazole. Brr2 used in RNA displacement assays was treated with TEV protease during overnight dialysis at 4 °C against 50 mM Hepes (pH 8.0), 10% (vol/vol) glycerol, 600 mM NaCl, 2 mM β-mercaptoethanol, and 15 mM imidazole to remove the N-terminal His$_{10}$-tag, and subsequently separated from the His-tagged TEV protease and the cleaved His$_{10}$-tag by recycling over a 5-mL HisTrap FF column. Brr2 used in all other experiments was not treated with TEV protease. The sample was then diluted to a final concentration of 70–80 mM NaCl and loaded on a HiPrep Heparin FF 16/10 column (GE Healthcare) equilibrated with 50 mM Tris·HCl (pH 8.0), 50 mM NaCl, 5% (vol/vol) glycerol, and 2 mM DTT. The protein was eluted with a linear gradient from 0.05 to 1.5 M NaCl and further purified by gel filtration on a 16/60 or 26/60 Superdex 200 column (GE Healthcare) run with 40 mM Tris·HCl (pH 8.0), 20% (vol/vol) glycerol, 200 mM NaCl, and 2 mM DTT.

DNA constructs encoding for yeast Snu13 and Prp3$^{296–469}$ were cloned into a pETM-11 vector (EMBL) for production of the targets as N-terminal His$_6$-tagged fusion proteins. DNA encoding yeast Prp31$^{2–388}$ was cloned into a pGEX-6P vector (GE Healthcare) for production of the target as an N-terminal, PreScission-cleavable GST fusion protein. The Snu13 and Prp31 plasmids were transformed into *E. coli* BL21 (DE3)-T1R cells. The Prp3 plasmid was transformed into *E. coli* BL21 (DE3)-RIL cells. Proteins were produced at 18 °C for 2 d using autoinduction media (59).

For purification of Prp3$^{296–469}$, a cell pellet of a 400-mL culture was resuspended and incubated for 1 h at 4 °C in 20 mM Tris·HCl (pH 7.0), 5% (vol/vol) glycerol, 300 mM NaCl, 30 mM imidazole, 10 mM $MgCl_2$, 5 mM β-mercaptoethanol, 2 μg/mL DNaseI, and 10 μg/mL lysozyme supplemented with EDTA-free protease inhibitor pills. Cells were lysed by sonication for 15 min in a Sonopuls Ultrasonic Homogenizer HD 3100 (amplitude of 60%, pulse on for 2.0 s, pulse off for 1.0 s). Prp3 was affinity-captured on a 5-mL HisTrap FF column equilibrated in 20 mM Tris·HCl (pH 7.0), 5% (vol/vol) glycerol, 300 mM NaCl, 30 mM imidazole, 10 mM $MgCl_2$, and 5 mM β-mercaptoethanol, and eluted with a linear gradient from 30 to 500 mM imidazole. A wash step with 1 M LiCl was included during the affinity chromatography to remove nucleic acids. Prp3 was further purified by gel filtration on a 16/60 Superdex 200 column equilibrated in 20 mM Tris·HCl (pH 7.0), 150 mM NaCl, and 2 mM DTT.

For purification of Snu13, a cell pellet of a 1-L culture was resuspended in 50 mM Hepes (pH 7.0), 500 mM NaCl, 15 mM imidazole, 0.05% Tween-20, 2 mM DTT, 5 μg/mL DNaseI, 10 μg/mL RNaseA, and 0.2 mg/mL lysozyme supplemented with EDTA-free protease inhibitor, and cells were lysed by sonication for 22 min in a Sonopuls Ultrasonic Homogenizer HD 3100 (amplitude of 80%, pulse on for 1.0 s, pulse off for 2.5 s). Snu13 was affinity-purified on a 5-mL HisTrap FF column equilibrated in 50 mM Hepes (pH 7.0), 500 mM NaCl, 15 mM imidazole, and 2 mM DTT. The protein was eluted with a linear gradient from 15 to 300 mM imidazole. The N-terminal His_6-tag was cleaved with TEV protease during overnight dialysis at 4 °C against 50 mM Hepes (pH 7.0), 500 mM NaCl, 10 mM imidazole, and 2 mM DTT, and then run again over a 5-mL HisTrap FF column. Snu13 used in on-column RNA displacement assays was not treated with TEV protease to keep the His_6-tag. The sample was then diluted to a final concentration of 120 mM NaCl for ion exchange chromatography on a HiPrep Heparin FF 16/10 column equilibrated in 50 mM Hepes (pH 7.0), 100 mM NaCl, and 2 mM DTT. The protein was eluted with a linear gradient from 0.1 to 1 M NaCl and further purified by gel filtration on a 16/60 or 26/60 Superdex 75 (GE Healthcare) column equilibrated in 10 mM Hepes (pH 7.0), 200 mM NaCl, and 2 mM DTT.

For purification of Prp31, a cell pellet of a 1-L culture was resuspended in 50 mM Hepes (pH 7.5), 600 mM NaCl, 5% (vol/vol) glycerol, 0.02% Triton X-100, 2 mM DTT, 5 μg/mL DNaseI, 10 μg/mL RNaseA, and 0.2 mg/mL lysozyme supplemented with EDTA-free protease inhibitor, and cells were lysed by sonication for 22 min in a Sonopuls Ultrasonic Homogenizer HD 3100 (amplitude of 80%, pulse on for 1.0 s, pulse off for 2.5 s). GST-Prp31 was affinity-captured using glutathione-Sepharose beads (GE Healthcare) equilibrated in 50 mM Hepes (pH 7.5), 600 mM NaCl, 5% (vol/vol) glycerol, and 2 mM DTT, and eluted in 50 mM Hepes (pH 7.75), 600 mM NaCl, 5% (vol/vol) glycerol, 2 mM DTT, and 20 mM glutathione. The N-terminal GST-tag was cleaved with PreScission protease during overnight dialysis at 4 °C against buffer containing 50 mM Hepes (pH 7.5), 200 mM NaCl, 5% (vol/vol) glycerol, and 2 mM DTT. Glutathione-Sepharose beads were used to separate the cleaved protein from the GST-tag and the GST-tagged PreScission protease. The sample was loaded on a HiPrep Heparin FF 16/10 column equilibrated in 50 mM Hepes (pH 7.5), 200 mM NaCl, 5% (vol/vol) glycerol, and 2 mM DTT; eluted with a linear gradient from 0.2 to 1 M NaCl in buffer containing 50 mM Hepes (pH 7.5), 5% (vol/vol) glycerol, and 2 mM DTT; and further purified by gel filtration on a 16/60 or 26/60 Superdex 75 column equilibrated in 10 mM Hepes (pH 7.5), 200 mM NaCl, 5% (vol/vol) glycerol, and 2 mM DTT.

RNA Production and Purification. U4 and U6 snRNAs and mutants thereof were in vitro-transcribed from PCR-amplified, linearized DNA fragments derived from recombinant pUC19 vectors containing the cloned U4, U6, or mutant genes for 4 h at 37 °C in 200 mM Tris·HCl (pH 7.5), 75 mM $MgCl_2$, 10 mM spermidine trihydrochloride, 50 mM NaCl, 100 mM NTPs (Jena Bioscience), 0.02 U/μL RNasin (moloX), 0.005 U/μL pyrophosphatase (Thermo Scientific), and 1.6 U/μL T7 RNA polymerase. In vitro-transcribed RNAs were treated with 0.02 U/μL DNaseI (Thermo Scientific) for 15 min at 37 °C. RNAs were then diluted in 35 mM Bis-Tris-Propane (pH 6.9), 50 mM NaCl, and 0.2 mM EDTA; loaded on a MonoQ 10/100 GL column (GE Healthcare) equilibrated in 35 mM Bis-Tris-Propane (pH 6.9), 200 mM NaCl, and 0.2 mM EDTA; and eluted with a linear gradient from 0.2 to 1.2 M NaCl. The sample was further purified by phenol-chloroform extraction using Roti-Aqua-P/C/I RNA extraction mix (Roth). Extracted RNAs were mixed with 10% (vol/vol) 3 M sodium acetate (pH 5.3) and precipitated with 1 vol of isopropanol for 20 min at −20 °C. The RNA pellets were washed with 70% (vol/vol) ethanol and dissolved in water.

UV Melting Analyses. Oligonucleotides for UV melting analyses were chemically synthesized. Absorbance versus temperature profiles were recorded at 250, 260, 270, and 280 nm on a Cary 100 spectrophotometer (Agilent) equipped with a multiple cell holder and a Peltier temperature control element. Samples were prepared at 1 μM RNA in unwinding buffer [40 mM Tris·HCl (pH 7.5), 50 mM NaCl, 0.5 mM $MgCl_2$] and measured in quartz cuvettes with a path length of 1 cm. Data were collected for two complete heating and cooling cycles (5–90–5 °C) at a rate of 0.7 °C for 1 min. Melting transitions were reversible at all four different wavelengths. Thermodynamic parameters were derived from two-state van't Hoff analysis of melting curves as described elsewhere (60).

RNA Labeling and Assembly of U4/U6 Di-snRNA and Di-snRNP. U4 and U6 snRNAs and mutants thereof were dephosphorylated with 0.27 U/μL Fast Alkaline Phosphatase (Thermo Scientific) in the manufacturer's buffer for 1 h at 37 °C and purified by phenol-chloroform extraction and isopropanol precipitation. Sixty picomoles of U4 RNAs were 5′–end-labeled with [γ-^{32}P]-ATP (PerkinElmer) using T4 polynucleotide kinase in the manufacturer's buffer (New England Biolabs) for 1 h at 37 °C. The labeling reaction was then loaded on a G25 spin column (GE HealthCare), and the labeled U4 RNA was recovered. Duplex annealing was carried out in 40 mM Tris (pH 7.5) and 50 mM NaCl in the presence of a fivefold molar excess of U6 RNA. The annealing mixture was incubated for 5 min at 80 °C and cooled to 70 °C, when the reaction was supplied with 10 mM $MgCl_2$. The reaction was further cooled to 25 °C over 1 h. The RNA duplex was separated from free U4 and U6 RNAs via 6% native PAGE run for 1 h at 200 V. The RNA duplex band was cut from the gel and eluted overnight in buffer containing 50 mM Tris (pH 7.5), 400 mM NaCl, 100 mM EDTA, and 0.5% SDS. Duplex RNA was then phenol-chloroform–extracted and isopropanol-precipitated. The duplex RNA pellets were washed with 70% (vol/vol) ethanol and subsequently dissolved in 40 mM Tris (pH 7.5) and 50 mM NaCl. The same steps were performed when U6 or mutant RNAs were 5′–end-labeled with [γ-^{32}P]-ATP.

U4/U6 di-snRNP assembly was initiated by incubation of U4/U6 di-snRNA with Snu13. Prp31, Prp3, and Brr2 alone or pre-assembled with Jab1$^{\Delta C}$ were added sequentially. Each incubation step was performed at 30 °C for 3 min.

Unwinding Assays. Helicase assays were performed at 30 °C for 0–68 min with 20 nM Brr2 alone or preassembled with 50 nM Jab1$^{\Delta C}$, 1.75 nM U4/U6 di-snRNA or mutants thereof, and optionally with 50 nM Snu13, 50 nM Prp31, and 50 nM Prp3 in unwinding buffer [40 mM Tris·HCl (pH 7.5), 50 mM NaCl, 8% (vol/vol) glycerol, 0.5 mM $MgCl_2$, 15 ng/μL acetylated BSA, 1 U/μL RNasin, 1.5 mM DTT]. The reactions were initiated by addition of 1.7 mM ATP/$MgCl_2$. Aliquots were taken at the indicated time points, and reactions were stopped by addition of 1 vol of stop buffer [40 mM

Tris·HCl (pH 7.4), 50 mM NaCl, 25 mM EDTA, 1% SDS, 10% (vol/vol) glycerol, 0.05% xylene cyanol, 0.05% bromophenol blue]. Samples were run on a 6% nondenaturing PAGE gel at 4 °C at 200 V for 1 h. RNA bands were visualized by autoradiography using a phosphor-imager (Molecular Dynamics) and quantified with Image Quant 5.2 software (GE Healthcare). Data were fit to a single exponential equation [fraction unwound = A{1 − exp ($-k_u$ t)}; A, amplitude of the reaction; k_u, apparent first-order rate constant of unwinding; t, time] using GraphPad Prism.

Gel-Based Protein Displacement Assays. Protein displacement assays were performed at 30 °C for 0–68 min with 400–800 nM Brr2 alone or preassembled with 1 μM Jab1$^{\Delta C}$, with 1.75 nM U4/U6 di-snRNA, 200 nM Snu13, 1 μM Prp31, and optionally 4 μM Prp3 in 40 mM Tris·HCl (pH 7.5), 50 mM NaCl, 8% (vol/vol) glycerol, 0.5 mM $MgCl_2$, 10–67 ng/μL heparin, 15–67.5 ng/μL acetylated BSA, 0–360 ng/μL yeast tRNA, 1 U/μL RNasin, and 1.5 mM DTT. To reduce unspecific binding and to resolve the band shifts well, the concentrations of heparin, acetylated BSA, and yeast tRNA were increased when more proteins were present in the assays. A total of 225 nM U4 snRNA or 1 μM U4 5′ SL (U4$^{20–53}$) trap was used in experiments containing radiolabeled U4 snRNA. Experiments containing U4 5′SL trap were performed with 30 nM Snu13 and 1.5 μM Brr2-Jab1$^{\Delta C}$. Experiments performed with radiolabeled U6 snRNA were done without U6 snRNA trap, because no rebinding of any of the proteins to U6 snRNA could be observed. The reactions were initiated by adding 1.7 mM ATP/$MgCl_2$ alone or premixed with trap RNA or with trap RNA alone (control). Aliquots were taken at the indicated time points, and reactions were stopped with 1 vol of stop buffer without SDS. Samples were loaded on a 4% nondenaturing PAGE gel containing 5% (vol/vol) glycerol and run at 170 V for 3–4 h. RNA bands were visualized as described above.

Column-Based Disruption Assays. All steps were performed at 30 °C. To monitor RNA displacement, 1.75 nM U4/U6 di-snRNA (U4 radiolabeled) was incubated with 200 nM His_6-tagged Snu13 and 1 μM Prp31 for 3 min in a total volume of 20 μL in unwinding buffer. Subsequently, the complex was immobilized for 6 min in 25 μL of Ni^{2+}-NTA agarose beads (Qiagen) preequilibrated in unwinding buffer and loaded on Pierce Micro-Spin Columns (Thermo Scientific). The on-column unwinding reaction was performed for 5 min with 20 μL of 1.7 mM ATP/$MgCl_2$ and 2.4 μM Brr2 alone, or optionally preassembled with 2.5 μM Jab1$^{\Delta C}$ in unwinding buffer. Elution of nondisplaced U4 snRNA and U4/U6 di-snRNA was performed for 5 min in 20 μL of 300 mM imidazole and 25 mM EDTA in unwinding buffer. Immobilization, unwinding, and elution steps were interspersed with two wash steps with 20 μL of unwinding buffer supplemented with 1 μM Prp31 to counteract spontaneous complex dissociation. After each incubation step, the solutions were recovered by centrifugation at 2,000 × g for 10 s in a 5415D tabletop centrifuge (Eppendorf). Fifteen microliters of the recovered solutions was mixed with 10 μL of stop buffer, and the samples were run on a 6% nondenaturing PAGE at 4 °C at 200 V for 1 h. RNA bands were visualized and quantified described as above.

Protein Labeling with Fluorescent Dyes. We exchanged a serine at position 93 of Snu13 for a cysteine because none of the other cysteine residues in WT Snu13 was accessible for labeling. In addition, we produced a Prp31$^{35–388}$ variant in which all cysteine residues had been exchanged with serines (C230S, C257S, C307S), except for an accessible cysteine at position 36. Snu13 and Prp31$^{35–388}$ variants were produced and purified like the WT proteins, except that the final buffer did not contain DTT. One hundred fifty micromolar proteins were preincubated with 500 μM Tris(2-carboxyethyl)phosphine hydrochloride (Sigma–Aldrich) for 10 min at 37 °C in labeling buffer [50 mM Hepes (pH 6.8), 200 mM NaCl]. Labeling was performed with 50 μM Cy3 or Cy5 maleimide monoreactive dye (GE Healthcare) in labeling buffer for 3.5 h. The reaction was stopped with 6 mM 2-mercaptoethanol (Merck). Labeled proteins were separated from the fluorescent dyes via gel filtration on a 10/300 Superdex 75 column (GE Healthcare) equilibrated in labeling buffer.

FRET-Based Disruption Assays. FRET-based stopped-flow measurements were performed on a SX-20 stopped-flow spectrometer (Applied Photophysics) at 30 °C in buffer containing 40 mM Tris·HCl (pH 7.5), 50 mM NaCl, and 0.5 mM $MgCl_2$. Cy3 fluorescence was excited at 530 nm, and its emission was measured after passing a 550-nm cutoff filter (Applied Photophysics). Cy5 was excited via FRET from Cy3 if labeled Snu13 and Prp31$^{35–388}$ were bound to U4/U6 di-snRNA. Cy5 fluorescence was monitored after passing a 645-nm cutoff filter (Applied Photophysics).

U4/U6 di-snRNP was assembled from 250 nM U4/U6 di-snRNA, 500 nM labeled Snu13, 250 nM labeled Prp31$^{35–388}$, 50 nM Brr2, and 50 nM Jab1$^{\Delta C}$. Brr2-Jab1$^{\Delta C}$–mediated disruption reactions were initiated by rapid mixing of 60 μL of the assembled complex with 60 μL of 1.7 mM ATP/$MgCl_2$ and 1.25 μM nonlabeled Prp31. The fivefold excess of nonlabeled Prp31 over labeled Prp31 was used to avoid rebinding of the labeled Prp31 variant. Fluorescence change time courses were averaged from at least four individual traces. Time-dependent FRET decrease rates were obtained by fitting the data to a single exponential equation [FRET = A{1 − exp($-k_u t$)}; A, amplitude of the reaction; k_F, apparent first-order rate constant of FRET decrease; t, time) using GraphPad Prism.

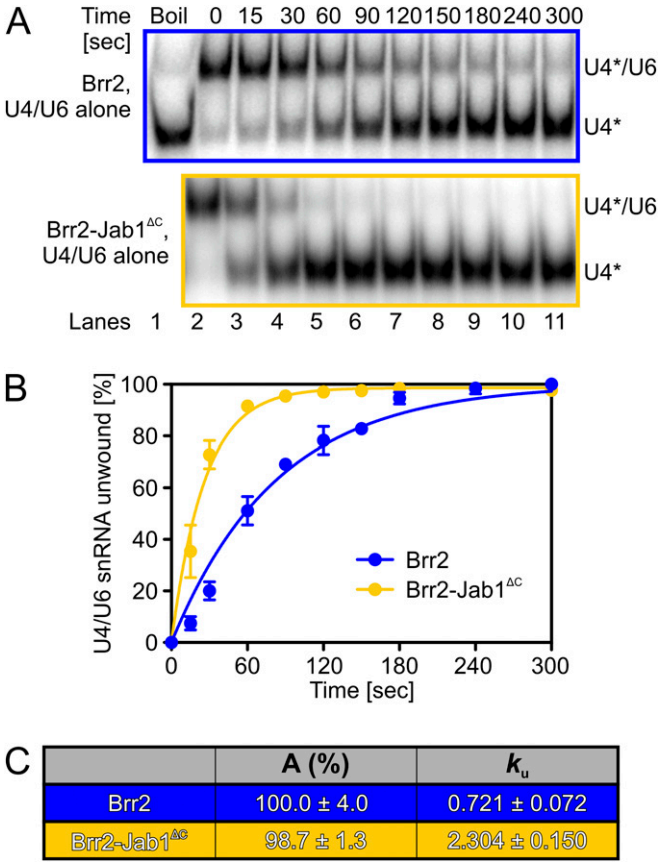

C

	A (%)	k_u
Brr2	100.0 ± 4.0	0.721 ± 0.072
Brr2-Jab1$^{\Delta C}$	98.7 ± 1.3	2.304 ± 0.150

Fig. S1. Jab1$^{\Delta C}$ enhances Brr2-mediated U4/U6 unwinding in the absence of U4/U6-bound proteins. (*A*) Gel analysis of Brr2- or Brr2-Jab1$^{\Delta C}$–mediated unwinding of U4/U6 di-snRNA. Time points are indicated above the gels, and bands are identified on the right. *Radiolabel. (*B*) Quantification of the data presented in *A*. (*C*) Data were fit to a single exponential equation [fraction unwound = A{1 − exp(−k_u *t*)}]. Data represent mean ± SEM of at least three independent experiments.

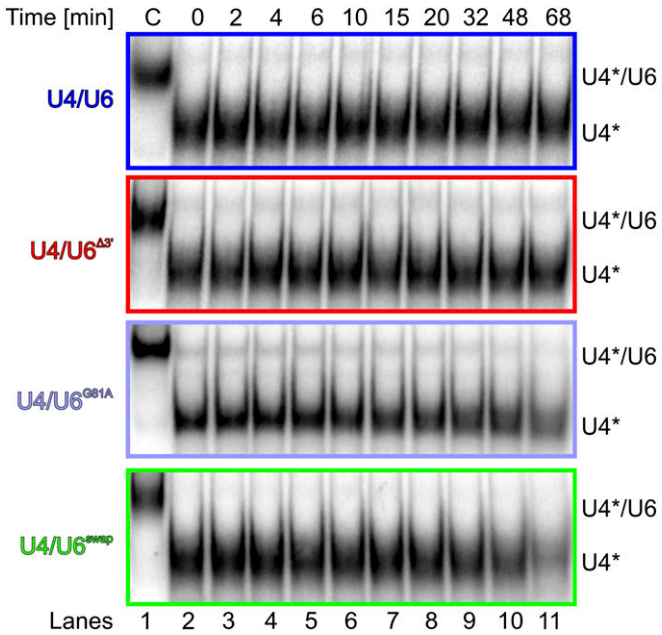

Fig. S2. Reannealing controls of WT and mutant U4 and U6 snRNAs. Gels monitoring the incubation of isolated WT or mutant U4 and U6 snRNAs (lanes 2–11) show that none of the snRNA combinations spontaneously anneal. C, control showing the migration of the respective wt or mutant duplexes (lane 1). Time points are indicated above the gels, and bands are identified on the right. *Radiolabel.

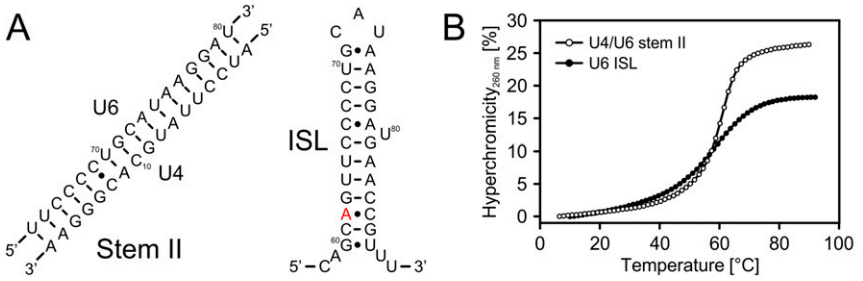

C

	U4/U6 stem II	U6 ISL
T_m [°C]	59.5 ± 0.5	58.3 ± 0.5
ΔH [kcal/mol]	-88.8 ± 5.2	-32.3 ± 1.8
ΔS [cal/mol/K]	-265 ± 12	-97 ± 5
ΔG [kcal/mol]	-8.9 ± 0.7	-3.2 ± 0.4

Fig. S3. Thermodynamic stabilities. (*A*) Sequences of U4/U6 stem II and U6 ISL. The exchange of residue A62 for G (red in the ISL structure) leads to a cold-sensitive phenotype and reduced U4/U6 levels due to hyperstabilization of the ISL. (*B*) UV melting curves. Hyperchromicity was calculated from absorbance at 260 nm and plotted vs. temperature for U4/U6 stem II and U6 ISL at 1 μM in unwinding buffer. Representative heating curves are shown. Heating and cooling curves showed reversible folding and unfolding. (*C*) Thermodynamic data were determined by van't Hoff analysis from two datasets of four melting curves each. ΔH and ΔS were determined at T_m, and ΔG was extrapolated to 298 K.

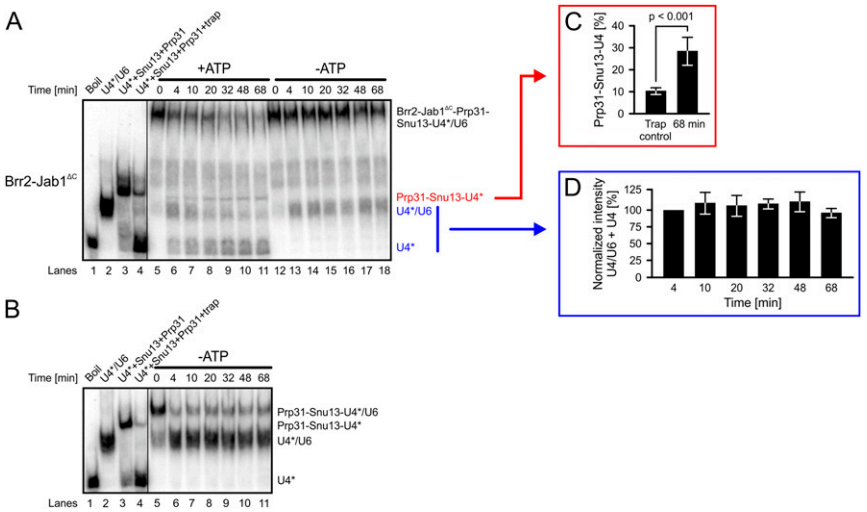

Fig. S4. Gel analysis of Brr2-mediated U4/U6 di-snRNP disruption. (*A*) Experiment is as in Fig. 3*A* but with smaller amounts of Snu13 and a large excess of U4 5′SL trap. Lanes 1–3, migration of RNAs and RNPs; lane 4, trapping control; lanes 5–18, time courses of Brr2-Jab1$^{\Delta C}$–mediated Prp31-Snu13-U4/U6 di-snRNP disruption in the presence (lanes 5–11) or absence (lanes 12–18) of ATP. Under these conditions, Prp31-Snu13-U4/U6 migrated as a complex with Brr2-Jab1$^{\Delta C}$ on the gels. (*B*) Control experiment showing that the high concentration of U4 5′SL trap disrupts part of the Prp31-Snu13-U4/U6 RNP. Lanes 1–3, migration of RNAs and RNPs; lane 4, trapping control; lanes 5–11, time course of Prp31-Snu13-U4/U6 di-snRNP disruption upon addition of U4 5′SL trap. Time points are indicated above the gels, and bands are identified on the right. *Radiolabel. (*C*) Quantification of U4 and Prp31-Snu13-U4 band intensities of lanes 4 and 11 of *A*, showing that more relative Prp31-Snu13-U4 RNP is formed during Brr2-Jab1$^{\Delta C}$–mediated unwinding than in the trap control experiment. Significance was assessed using an unpaired Student's *t* test. (*D*) Combined U4/U6 and U4 in lanes 6–11 of *A* normalized to band intensities of U4/U6 and U4 in lane 6. Data represent mean ± SEM of four independent experiments.

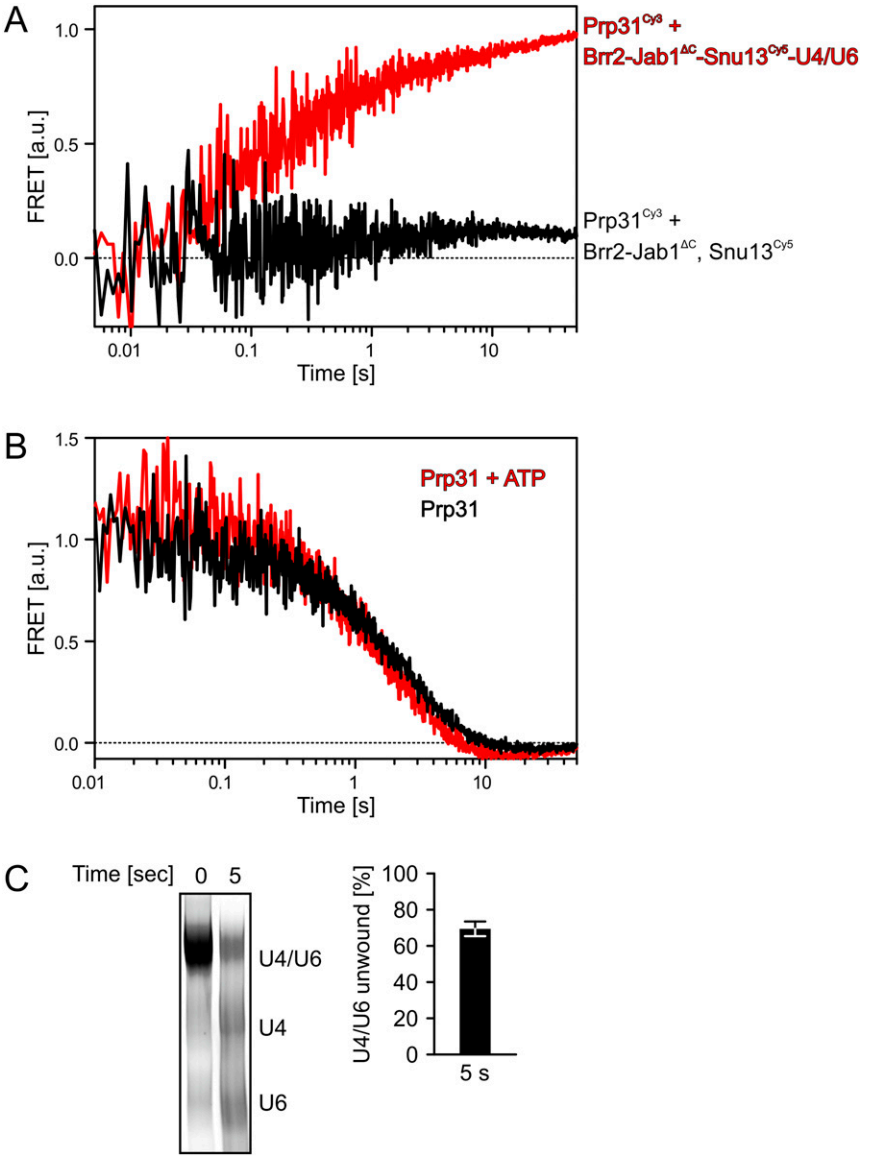

Fig. S5. FRET-based assay monitoring Brr2-mediated U4/U6 di-snRNP disruption using a stopped-flow apparatus. (*A*) Binding of Prp31^{Cy3} to Brr2-Jab1$^{\Delta C}$-Snu13^{Cy5}-U4/U6 (red curve) gave rise to FRET signal, whereas no signal was observed upon mixing Prp31^{Cy3}, Snu13^{Cy5}, and Brr2-Jab1$^{\Delta C}$ in the absence of U4/U6 di-snRNA (black curve). a.u., arbitrary units. (*B*) Addition of a fivefold excess of unlabeled Prp31 to a Brr2-Jab1$^{\Delta C}$-Prp31^{Cy3}-Snu13^{Cy5}-U4/U6 RNP led to a time-dependent decrease of the FRET signal, representing spontaneous dissociation of Prp31^{Cy3} and its replacement by unlabeled Prp31 (black curve). Prp31^{Cy3} dissociation rates were similar in the presence of ATP (FRET decrease rate in the absence of ATP = 0.40 ± 0.007 per second; FRET decrease rate in the presence of ATP = 0.55 ± 0.009 per second). For each experiment, four traces were averaged and fit to a single exponential equation to obtain the FRET reduction rates and their respective SEs. (*C*) Brr2-Jab1$^{\Delta C}$–dependent disruption of a Prp31^{Cy3}-Snu13^{Cy5}-U4/U6 RNP within 5 s. (*Left*) Gel monitoring disruption under conditions identical to the conditions used for the FRET assays. Due to the large volumes and high RNA concentrations, disruption was monitored by methylene blue staining of the gel. (*Right*) Quantification of the fraction of Prp31^{Cy3}-Snu13^{Cy5}-U4/U6 RNP disrupted after 5 s. Due to possible differential staining of single- and double-stranded RNAs, quantification was based on the reduction of the U4/U6 band. Data represent mean ± SEM of four independent experiments.

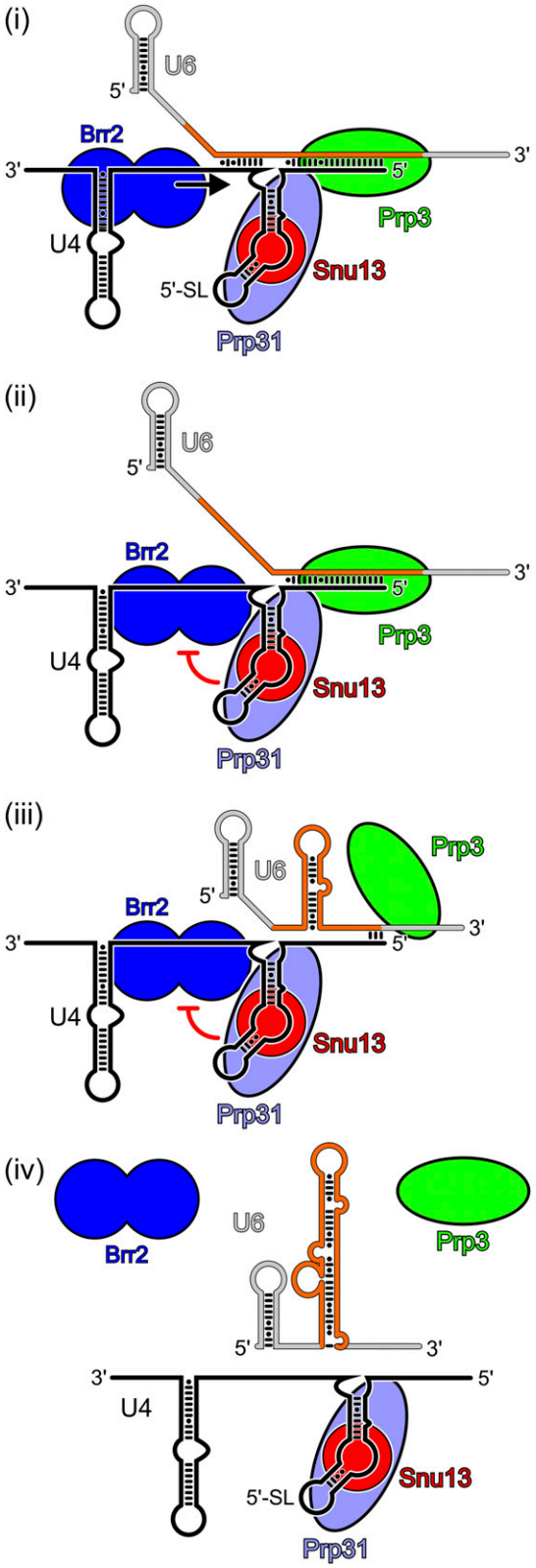

Fig. S6. Model of Brr2-mediated U4/U6 di-snRNP disruption. (*i*) Brr2 binds to a single-stranded region of U4 snRNA and unwinds U4/U6 stem I (black arrow). (*ii*) Kink in U4 snRNA and/or the tightly bound Snu13 and Prp31 proteins prevents Brr2 from translocating into the U4 5′SL (red symbol). (*iii*) Unwound U6 snRNA regions induce formation of an alternative U6 structure, dismantling the Prp3-binding site. (*iv*) Brr2 disengages from U4 snRNA, yielding a Prp31–Snu13–U4 snRNA complex, free Prp3, and free U6 snRNA.